

AD-A090 404

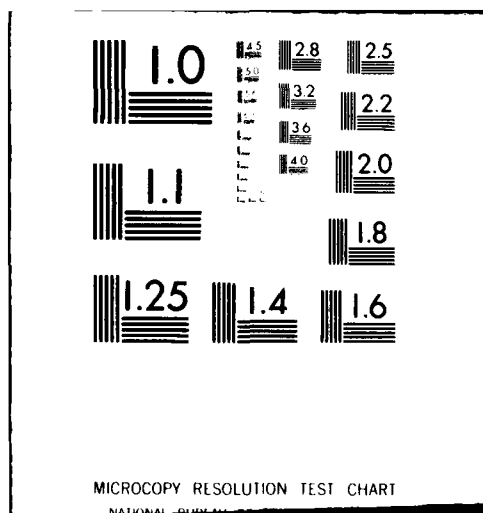
ARMY ARMAMENT RESEARCH AND DEVELOPMENT COMMAND ABERD--ETC F/G 20/6
INFRARED TRANSMISSION MEASUREMENTS THROUGH SCREENING SMOKES: EX--ETC(U)
JUN 80 6 C HOLST

UNCLASSIFIED

NL

For I
ARDC
Aberd

END
DATE
FILED
11-80
DTIC



AD A090404

DDC FILE COPY

HOLST

LEVEL II
①

INFRARED TRANSMISSION MEASUREMENTS THROUGH
SCREENING SMOKES: EXPERIMENTAL CONSIDERATIONS

JUN 1980

GERALD C. HOLST, Ph.D.
CHEMICAL SYSTEMS LABORATORY, USAARRADCOM
ABERDEEN PROVING GROUND, MD 21010

I. INTRODUCTION

In order to evaluate the effect of tactical screening smokes on infrared transmission, it is necessary to understand the complex interactions among many variables. The transmission depends upon the bulk properties of the material (e.g., index of refraction), as well as the particle-size distribution, concentration, and pathlength. The measured or apparent transmission can be quite different from the true transmission because several simple basic facts are often overlooked. Therefore, it becomes quite difficult to compare data from different laboratories or from field tests because the experimental methodology is different at each location.

In principle, it is possible to calculate the transmission of the smoke if the particle-size distribution, concentration, pathlength, and the complex index of refraction are known. But these parameters are not always known precisely, and one resorts to experimentation to define them. The experiment becomes that of introducing a smoke with unknown infrared properties between the target and the detector. The ratio of the signal received with smoke to that without smoke is taken as the transmission.

In addition to transmissometers, the effects of screening smokes on thermal imaging systems is of interest. The experiment is similar to the transmissometer test. A smoke is introduced until the target can no longer be perceived by an observer. The amount of smoke required is a measure of the smoke's obscuring power. A second type experiment consists of introducing a "standard" smoke between several

DTIC

247

This document has been approved
for public release and sale; its
distribution is unlimited.

275

80 10 16 037

different imaging systems and a target. The concentration is increased until the target has disappeared on several imaging systems. At this point, certain conclusions are drawn about the smoke's screening effectiveness, but the results may be a measure of the system's behavior and the observer's ability rather than the smoke's effectiveness.

Presented in sections II through V are the basic principles that the experimentalist should consider before designing the experiment.

II. Laser Transmission and Scattering

Using Beer's law it is possible to calculate the transmission of an aerosol when the mass extinction coefficient α , the concentration C , and the pathlength L are known:

$$T = \text{EXP} \left[- \int_0^L \alpha C(\lambda) d\lambda \right] \quad (1)$$

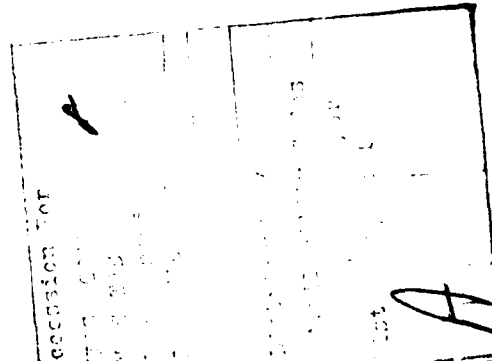
Assuming spherical particles, α can be calculated from the Mie scattering theory:

$$\alpha = \frac{3}{4\rho} \int_r Q(m, r/\lambda) \frac{N(r)}{r} dr \quad (2)$$

where Q is the Mie scattering factor, ρ is the mass density, m is the complex index of refraction, r is the radius of aerosol particle, λ is the wavelength, and $N(r)$ is the number density size distribution. The reason that α is usually obtained experimentally is that often neither m nor $N(r)$ is known. From equation (2), it follows that, if the size distribution changes, then α will change also. Any dynamic process, such as coagulation, sedimentation, or introduction of a new aerosol with a different size distribution, will change $N(r)$. For hygroscopic smokes, such as phosphorus and HC, the size distribution will depend upon the relative humidity and hence, α will be a function of relative humidity.

In recent experiments, fog oil smoke was produced by a vaporization condensation method. A laser transmissometer operating at $\lambda = 0.6328 \mu\text{m}$ measured the transmission as a function of time as shown in figure 1. The concentration was simultaneously obtained as shown in figure 2. The size distribution was obtained with cascade impactors at time $t = 0.0 \text{ min}$ and $t = 51 \text{ min}$. The mode diameter increased and the total number of particles greater than $2.0 \mu\text{m}$ actually increased, suggesting that coagulation has occurred. Thus $N(r)$ is changing with time. Using the data in figures 1 and 2, the extinction coefficient was calculated and is plotted in figure 3.

(276)



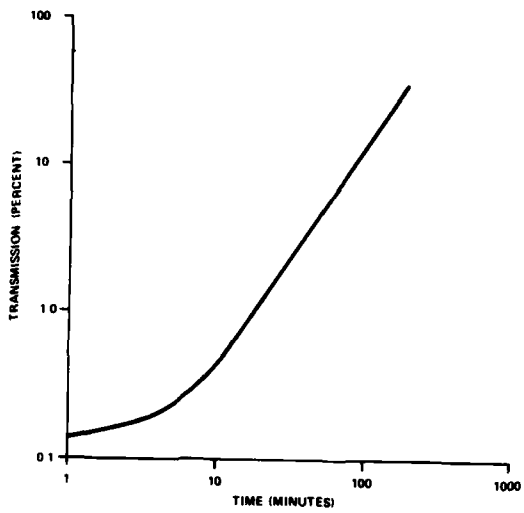


FIGURE 1. Transmission of a fog oil smoke as a function of time. Data obtained with a HeNe laser transmissometer ($\lambda = 0.6328 \mu\text{m}$). Laser pathlength was 1.2 m. Since the transmission is changing with time, some type of dynamic process is occurring.

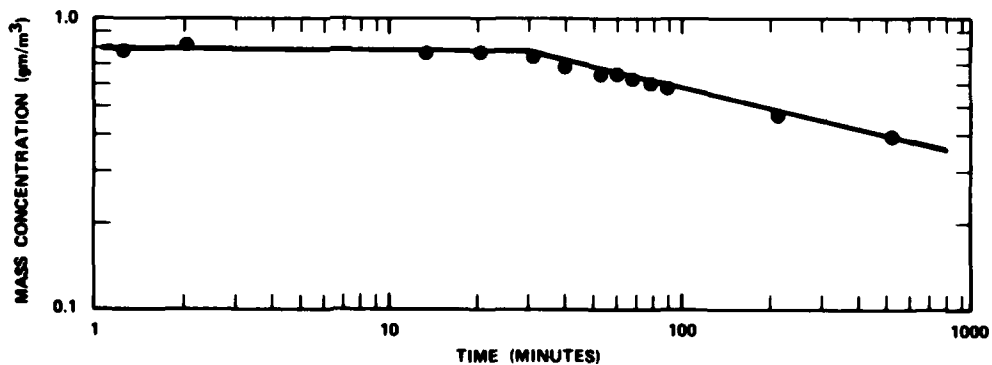


FIGURE 2. Mass concentration of a fog oil smoke as a function of time. Data obtained by gravimetric analysis of glass fiber filters. The aerosol was aspirated for 1 minute for each sample. The aerosol is stable for the first 20 minutes.

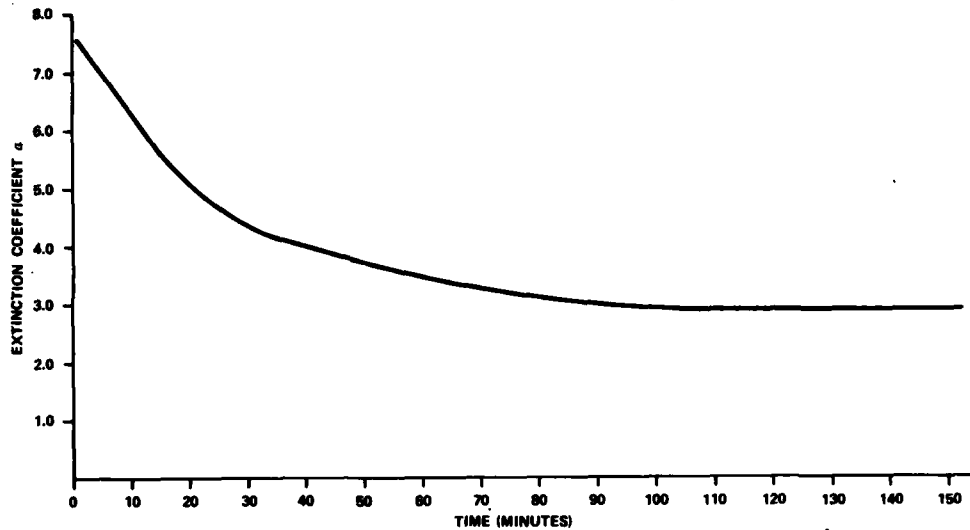


FIGURE 3. Calculated extinction coefficient as a function of time for a fog oil smoke. The transmission data shown in Figure 1, mass concentration data shown in Figure 2 and the pathlength $L = 1.2$ m was used in Beer's law. Since α is a function of time, the age of the cloud is significant when specifying α

As a general rule, coagulation becomes significant when the number density exceeds 10^6 particles/cm³ and the diameter is less than 1 μm . Sedimentation, on the other hand, dominates when $D > 1 \mu\text{m}$ in a chamber.

The extinction coefficient derived from Mie theory calculations assumes that any light scattered out of the incident beam contributes to total extinction. These calculations generally assume that the incident beam is a plane parallel wave of infinite extent and that the detector field of view (FOV) is essentially zero. In reality, the signal detected will depend upon how much scattering has taken place. Middleton⁽¹⁾ has shown that even for the single scattering case the amount of detected scattered light increases significantly as the detector FOV increases.

For dense aerosols, multiple scattering can occur. Second-order forward scattering has been treated theoretically⁽²⁾. The results indicate that, for typical polydisperse naturally occurring aerosols, a correction factor can be applied to the measured transmission to obtain the true extinction. The factor R which is a function of FOV,

size distribution and index of refraction appears in Beer's law as

$$T_{\text{measured}} = e^{-\alpha_m CL} = e^{-R \alpha_T CL} \quad (3)$$

where

$$R = \frac{\alpha_{\text{Measured}}}{\alpha_{\text{True}}} = \frac{\alpha_m}{\alpha_T} \quad (4)$$

Mooradian et. al.⁽³⁾ have shown that the detected signal is a function of receiver FOV for naturally occurring fogs. (See figure 4).

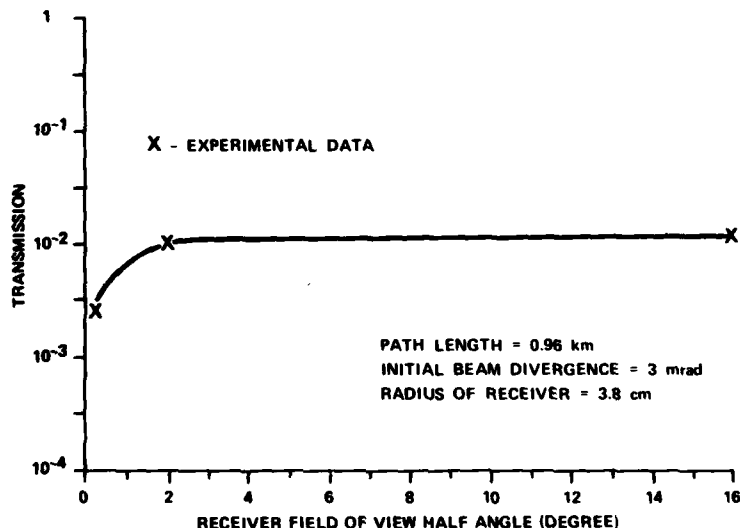


FIGURE 4. Measured transmission as a function of receiver field of view for naturally occurring water fogs (from Reference 3). The optical depth $\tau = 11.3$. The fog was not homogeneous. The laser transmissometer was a frequency doubled Q-switched Nd: YAG laser ($\lambda = 0.53 \mu\text{m}$). The solid line is the theoretical prediction which includes multiple scattering for dense aerosols.

III. Broadband Detectors: Spectral Response Consideration

The extinction coefficient, as shown in equation 1, is, in general a function of wavelength. For broadband detectors, the measured extinction is a function of the source temperature and the detector spectral response, as well as the spectral transmission of the smoke. The total flux reaching a detector from a target with emissivity ϵ_T at a single wavelength is given by

$$F_{OT} = T_a \epsilon_T R_T + L_a \quad (5)$$

where T_a is the transmission of the intervening atmosphere, R_T is the blackbody power emitted by the target, and L_a is the radiance of the atmosphere. When an emissive smoke is introduced, the flux reaching the detector becomes

$$F_{ST} = S a T^T \epsilon_T R_T + L_a^1 + T_a^1 R_s \quad (6)$$

where T_s is the transmission of the smoke, L_a^1 is the radiance modified by the smoke, and T_a^1 is the transmission of the atmosphere between the smoke and detector. R_s is a combination of the flux emitted by the smoke and the flux reflected off the cloud from external sources.

The current signal generated by these fluxes is given by $I=SF$, where S is the sensitivity of the detector. For broadband detectors the detector integrates over the wavelength of interest so that

$$I = \int_S F d\lambda \quad (7)$$

With synchronous detection, the source is modulated at some frequency and the detector electronics are sensitive to this frequency only. The path radiance and smoke emission are DC components and therefore are not measured. The measured ratio of smoke to no-smoke currents becomes

$$\langle T \rangle = \frac{I_{ST}}{I_{OT}} = \frac{\int_S T^T \epsilon_T R_T d\lambda}{\int_S T_a^1 R_s d\lambda} \quad (8)$$

$\langle T \rangle$ is the spectral averaged transmission and depends upon the spectral character of S , T_a , R_T , and T_s .

The effect of spectral mismatch between the smoke and the detector only is shown in the following exaggerated example. Consider four different hypothetical systems, all of which are nominally classified as 8 to 14 μm radiometer-transmissometer systems. The spectral sensitivity of each is shown in figure 5. Consider a screening agent whose transmission is 80% from 8 to 11 μm and from 100% from 11 to 14 μm for unit pathlength and unit concentration. As the smoke concentration increases, the transmission in the 11 to 14 μm stays at 100%, and the transmission from 8 to 11 μm approaches zero. Thus, as far as detector 2 is concerned, the smoke is transparent. Since detector 1 integrates over the entire region, the transmission approaches 50% and with detector 4, the transmission goes to zero. Detector 3 shows some intermediate value. In figure

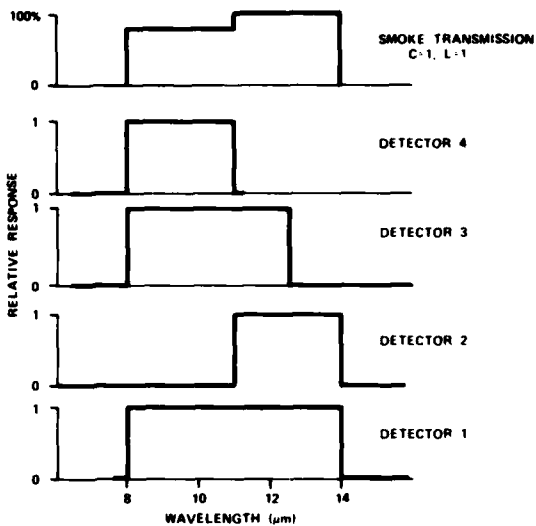


FIGURE 5. Spectral response of four hypothetical detectors. The relationship between these detectors and a hypothetical smoke is shown.

6, the expected transmission for each of these detectors is plotted as a function of concentration. The values were calculated with equation 8 and by letting $R_T = \epsilon_T = T_a = 1$. Although this example was exaggerated, the shape of the hypothetical smoke transmission is somewhat similar to phosphorus smoke (4,5)

The effect is not limited to the spectral mismatch of the smoke and detector. The spectral emission of the target (source) will also affect the measured transmission or extinction coefficient. Assuming that the source is a blackbody, calculations indicate that if a broadband HgCdTe detector is used, the measured transmission will decrease from 45% to 39% as the blackbody temperature is increased from 300°K to 1000°K.

Thus it is easy to see that there is no simple way of obtaining the smoke transmission with a broadband detector because of the measured transmission depends upon the target temperature, spectral response of the detector, and the atmospheric transmission. The atmospheric transmission is a function of pathlength, relative humidity, temperature, and local naturally occurring aerosols.

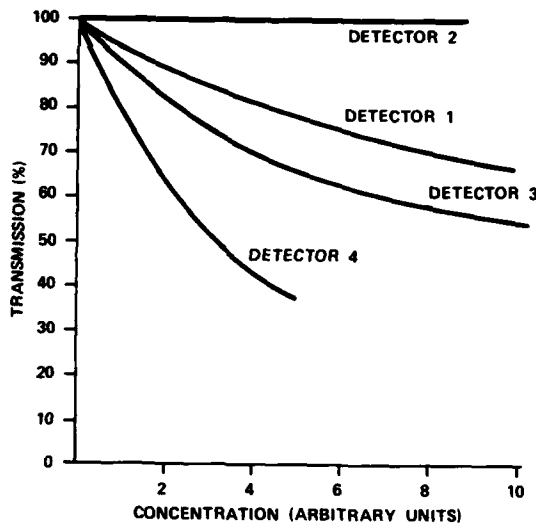


FIGURE 6. Calculated transmission as a function of concentration. The extremely large difference in transmission between detector 2 and detector 4 illustrates why spectral responses must be considered before collecting data.

IV. Imaging Systems: Minimum Resolvable Temperature Considerations

The imaging systems, in addition to having the same limitations as discussed in the preceding sections, also rely upon the observer's evaluation of the image. As mentioned when evaluating the effectiveness of a smoke, the smoke concentration is increased until an observer can no longer detect the target. At this point, the target signature is below the internal noise of the entire detector-electronics-human observer system.

The noise level is referred back to the input as an equivalent temperature and is specified as the minimum resolvable temperature (MRT) above ambient for a "standard" observer and is expressed as a temperature differential ΔT above ambient. The MRT is a function of the angular subtense α of the target and is plotted for two systems in figure 7. These systems are identical in the sense that for all targets larger than α they exhibit the same MRT. At another target angular subtense α_1 , the MRT of the two systems are given by ΔT_{N1} and ΔT_{N2} respectively. Assume that a target is presented before these two systems and it is ΔT above the ambient. If an absorbing smoke is placed between the detectors and the target, then, since ΔT_1 is larger than ΔT_2 , more smoke is needed to bring the target signature below the

HOLST

MRT for system 1 than for system 2.

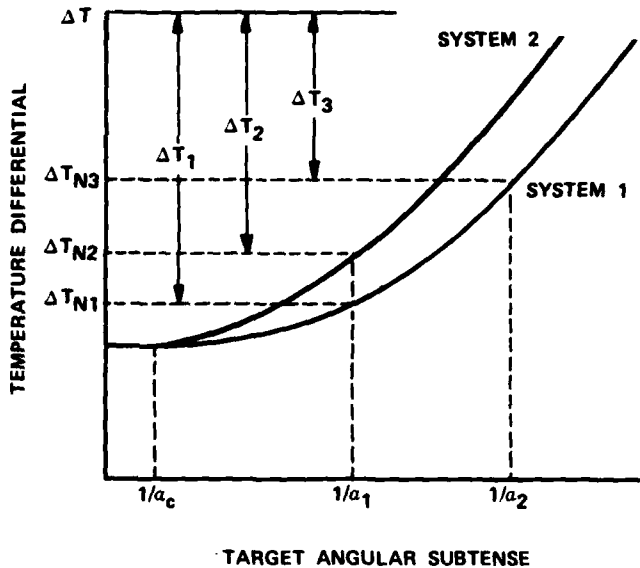


FIGURE 7. Minimum resolvable temperature of two hypothetical imaging systems as a function of target angular subtense.

Consider instead that, during two different tests, only system 1 is used and the target sizes are slightly different (a_1 and a_2). Since ΔT_1 is greater than ΔT_3 , more smoke is needed to obscure target size a_1 . During field smoke trials, actual military targets (tanks, trucks, etc.) are used. The equivalent ΔT of the target depends upon the emissivity, target temperature, target size, and the spatial distribution of the heat (e.g., the engine area will be the hottest area). An equivalent ΔT is calculated so that the MRT can be used to describe system performance. Since the spatial distribution of the heat and the temperature can change from test to test, it is easy to see that the equivalent ΔT will change. Therefore, it becomes exceedingly difficult to compare field data. Conclusions reached about the effectiveness of smoke may result from differences in the detector MRT or target equivalent ΔT rather than the optical properties of the smoke.

In many field tests, trained observers are not used. The relationship between a trained observer and a casual observer is not clear. This is extremely important because the systems are characterized by how well a trained observer can perceive targets.

V. Target Obscuration

Consider, now, an imaging device which processes the detected flux into various gray levels to produce an image on a TV screen. Let us assume that the device is adjusted so that, before the smoke is introduced, the hot target will appear as pure white and the background will appear as black. Let us assume that the device will insert 10 gray levels between these points so that each gray level is proportional $(I_{OT} - I_{OB})/10$ where I_{OB} is the background signal without smoke.

Before any further analysis is possible, the exact mode of operation of the thermal imaging system must be known. There are two basic modes. In the first, the instrument is adjusted for optimum display and the controls are not further adjusted, even after the smoke is introduced. In the second mode, the internal automatic gain control (AGC) automatically adjusts the gain so that an optimum display is always present. The first mode is typical of laboratory-type systems and the second is typical of military imaging systems.

Let us first consider a device which will not be readjusted. There are three possible conditions which will obscure the target as shown in figure 8. If the flux differential between target and background is very small, then a relatively high transmission will obscure a target in A. In B very little emission/reflection energy is necessary to make the entire screen white.

In C, the relationship between emission/reflection and attenuation causes the image to disappear into a gray level and then the entire screen will be gray. Then

$$I_{ST} - I_{SB} \leq \frac{I_{OT} - I_{OB}}{10} \quad (9)$$

This results in an averaged transmission (T) $< 1/10$. It indicates that the observer will be unable to see his target everytime the spectral averaged transmission drops below 10% for a 10 gray level system provided that he does not readjust his thermal imaging system. If the system is not optimized, i.e., both the background and target are in the gray levels, then the relationship presented above is relaxed in the same sense that a higher transmission smoke will produce the same effect. Thus, the three cases presented are "worst" cases.

Consider, now, the device which has an AGC or one that is readjusted for optimum display after the smoke is present. The only inequality that exists is when the attenuation and emission-reflection combined produces a signal differential between the target and back-

ground that is below the equivalent noise, current, I_N :

$$I_{ST} - I_{SB} \leq I_N \quad (10)$$

We can represent this current as an equivalent blackbody R_N with emissivity $\epsilon = 1$, and a temperature differential ΔT_N above the ambient. Full analysis indicates that

$$\langle T^4 \rangle < \frac{\Delta T_N}{\Delta T} \quad (11)$$

which is the well-known equation that indicates the spectral average smoke transmission must be sufficiently small to reduce the target-background differential below the MRT of the imaging system. This average $\langle T^4 \rangle$ is different from that defined by equation 8.

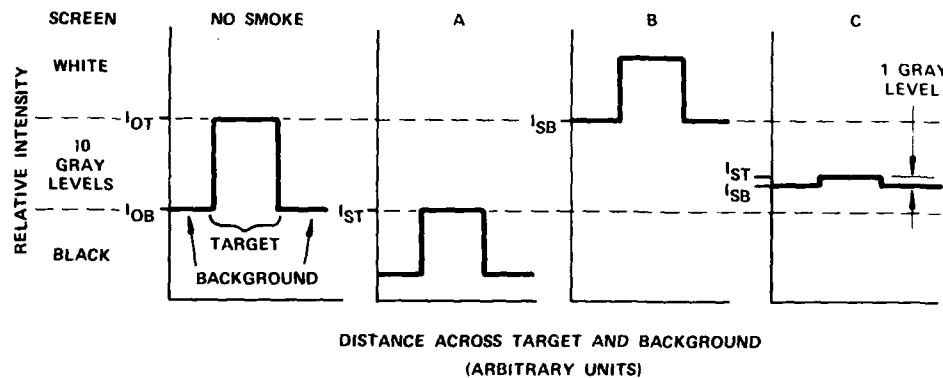


FIGURE 8. Three methods of obscuring a target detected with a thermal imaging system. With no smoke the target is pure white and the background is pure black. In A, smoke reduced the target signature below the black level. In B, the smoke emission/reflection raised the background into the white level. In C, emission/reflection combined with attenuation put the target-background intensity differential into a gray level.

For both systems (e.g., with ACG and without) we have assumed that the emissivities were equal to one and that the blackbody flux was wavelength independent and proportional only to the temperature. In practice, however, none of the assumptions are truly valid, and, therefore, we must consider the conclusions as guidelines rather than as facts.

Because of all the problems associated with thermal imaging systems, they should not be used to quantify the effectiveness of smoke. Rather they should be used solely for qualitative purposes.

VI. Conclusions

The various difficulties encountered in measuring transmission of aerosols have been discussed. Specifically, scattered light, whether single or multiple, can enter a large FOV detector and give an artificially high transmission. Any dynamic process, such as sedimentation and coagulation, can alter the size distribution and thereby alter the results of transmission measurements. For aerosol measurements to be reproducible, it is necessary to generate exactly the same size distribution and concentration each time. A flow chart indicating possible errors in laser transmissometer measurements is shown in figure 9.

To intelligently analyze data from broadband detectors, the spectral components of the target, smoke, intervening atmosphere, and the detector must be known. To obtain consistent results, in addition to the aerosol reproducibility requirements, the target temperature and intervening atmosphere must always be the same. For small pathlengths, the atmospheric transmission is near 100%; however, for long pathlengths, transmission depends upon relative humidity, temperature, and atmospheric constituents, all of which can vary on an hourly basis. If two different detectors are used, the spectral responses must be identical. The flow chart illustrating these problems is shown in figure 10.

Field measurements are extremely difficult because the local meteorological conditions can disperse the cloud and create inhomogeneities in concentration. Furthermore, recent evidence suggests that fog oil droplets may partially evaporate. In that case since r is decreasing, even the extinction coefficient will change.

Finally, for target obscuration with a thermal imaging system with an AGC, sufficient smoke must be present to reduce the target-background temperature differential below the MRT of the system. The MRT depends upon the angular subtense of the target. The problems inherent to broadband detectors and transmissometers also apply. The flow chart is shown in figure 11. Note that only trained observers should be used if the only information available is the display screen.

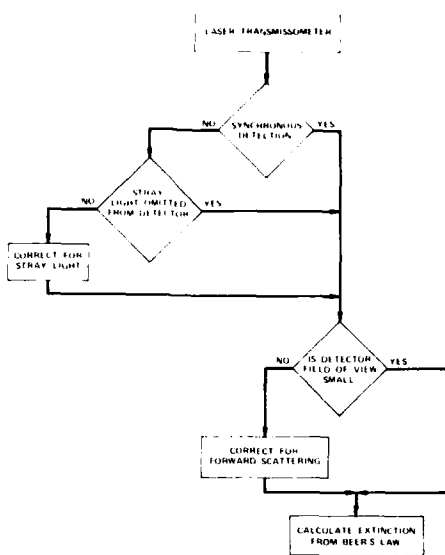


FIGURE 9. Flow chart of possible experimental errors encountered with laser transmissometers.

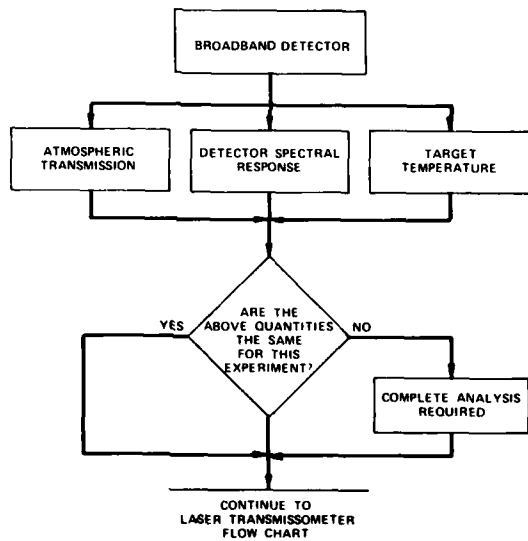


FIGURE 10. Flow chart of possible experimental errors encountered with broadband detectors.

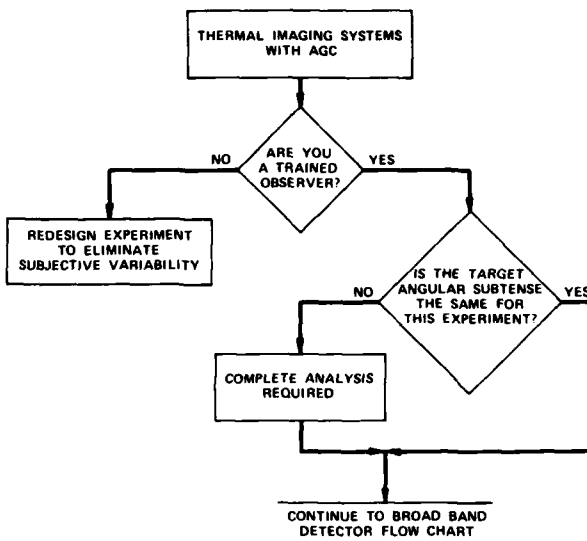


FIGURE 11. Flow chart of possible experimental errors encountered with thermal imaging systems.

References

1. W. E. K. Middleton. Vision Through the Atmosphere, University of Toronto Press, 1952, pg 177.
2. A. Deepak and M. A. Box, "Forward Scattering Corrections for Optical Extinction Measurements in Homogeneous Polydisperse Aerosols", Applied Optics, 17, 3169, 1978.
3. G. C. Mooradian, M. Geller, L. B. Stotts, D. H. Stephens, and Drantwald, "Blue-Green Pulsed Propagation Through Fog", Applied Optics, 18, 429, 1979.
4. M. Milham, "A Catalog of Optical Extinction Data for Various Aerosol/Smokes", ED-SP-77002, June 1976.
5. G. C. Holst and M. E. Milham, "Examination of the Correlation between Laboratory and Field Smoke Extinction Data", in Proceedings of the Smoke Symposium, HDL, April 1979.

